

 Open access • Journal Article • DOI:10.1109/10.237693

## Excitation of dorsal root fibers in spinal cord stimulation: a theoretical study

— [Source link](#) 

Johannes J. Struijk, J. Holsheimer, Herman B. K. Boom

**Published on:** 01 Jul 1993 - IEEE Transactions on Biomedical Engineering (IEEE)

**Topics:** A delta fiber and Spinal cord

Related papers:

- [Recruitment of dorsal column fibers in spinal cord stimulation: influence of collateral branching](#)
- [Analysis of Models for External Stimulation of Axons](#)
- [Paresthesia thresholds in spinal cord stimulation: a comparison of theoretical results with clinical data](#)
- [Analysis of a Model for Excitation of Myelinated Nerve](#)
- [Which elements are excited in electrical stimulation of mammalian central nervous system: a review](#)

Share this paper:    

View more about this paper here: <https://typeset.io/papers/excitation-of-dorsal-root-fibers-in-spinal-cord-stimulation-1jw035fnp7>

# Excitation of Dorsal Root Fibers in Spinal Cord Stimulation: A Theoretical Study

Johannes J. Struijk, Jan Holsheimer, and Herman B. K. Boom

**Abstract**—In epidural spinal cord stimulation it is likely that not only dorsal column fibers are activated, but that dorsal root fibers will be involved as well. In this investigation a volume conductor model of the spinal cord was used and dorsal root fibers were modeled by an electrical network including fiber excitation. The effects of varying some geometrical fiber characteristics, as well as the influence of the dorsal cerebrospinal fluid layer and the electrode configuration on the threshold stimulus for their excitation, were assessed.

The threshold values were compared with those of dorsal column fibers. The results of this modeling study predict that, besides the well known influence of fiber diameter, the curvature of the dorsal root fibers and the angle between these fibers and the spinal cord axis were of major influence on their threshold values. Because of these effects, threshold stimuli of dorsal root fibers were relatively low as compared to dorsal column fibers. Excitation of the dorsal root fibers occurred near the entry point of the fibers.

## I. INTRODUCTION

VARIOUS effects of epidural spinal cord stimulation (ESCS) have been reported in the literature. With dorsal electrode placement the immediate effects are paresthesia (felt as tingling on the skin) and muscle contractions. Sometimes therapeutic effects can also be achieved instantly. Shealy *et al.* [1], [2] reported immediate pain relief whereas Barolat [3] found a reduction of spasm and clonus within a second after onset of the stimulation.

Although paresthesia often starts as segmental sensations, it spreads to dermatomes corresponding with low spinal levels when the stimulus amplitude is increased [2], [4], [5]. In contrast, muscle contractions are typically a segmental effect of dorsal ESCS [4], [5] which, with increasing amplitude, only spreads to adjacent spinal levels [4]. In ESCS at a midthoracic level, a segmental band of muscle contractions around the thorax often occurs at a slightly higher stimulus than (or even below) the sensory threshold, thus preventing a satisfactory therapeutic effect.

Dimitrijevec *et al.* [4] supposed that the dorsomedial column fibers (DC fibers) are activated first and then, with increasing stimulus amplitude, activation occurs deeper and more laterally in the dorsal columns, also reaching the dorsal roots and their entry zones. They attributed immediate motor responses to the activation of primary afferents at the dorsal root entry zone,

thus activating motoneurons by spinal reflex pathways. Direct stimulation of ventral root (motor) fibers or alpha-motoneurons in the ventral horn is not a probable mechanism since in dorsal ESCS motor responses do not follow a stimulus pulse train beyond 20 pps, while in ventral stimulation they do so up to 100 pps. The measured latency of the responses also favors reflex activity as the explanation for motor responses [5].

These results favor the hypothesis, based on a theoretical study by Coburn [6], that dorsal root fibers (DR fibers) have lower thresholds than DC fibers with the same diameter, because of the curvature of the DR fibers. The immediate segmental effects may thus imply not only that DC fibers are activated in dorsal ESCS, but that DR fibers are involved as well. Coburn compared the excitation thresholds of DR fibers of 2.5- $\mu\text{m}$  diameter, having various curvatures, and DC fibers of 2, 5, and 10  $\mu\text{m}$  at several positions in the dorsal columns. The DC fibers were supposed to be in a transverse plane at the level of the cathode and to terminate in the dorsal columns, while the DR fibers were supposed to be simple straight rostrocaudal ones. Because of these simplifications, conclusions from this work should be drawn with care. As computed by Struijk *et al.* [7], the addition of collaterals to a DC fiber diminishes the excitation threshold up to 50% in this kind of fiber model.

In the present work we compared the excitation thresholds of DC fibers having collaterals with the thresholds of DR fibers having a realistic curvature in the transverse plane and in the rostrocaudal direction. Attention was also paid to the influence of the rostrocaudal level of the DR fiber as compared to the level of the electrodes, the fiber diameter, the positions of the nodes of Ranvier, the electrode configuration (monopolar and bipolar) and the thickness of the cerebrospinal layer between the electrodes and the dorsal columns.

The potential field imposed by the stimulation was calculated using an inhomogeneous volume conductor model [7], [8]. This field was used to calculate the excitation threshold stimuli in McNeal-like models [7], [9] of DC fibers and DR fibers and to predict at which part of the DR fibers excitation will be initiated.

## II. VOLUME CONDUCTOR MODEL

A transverse section of the volume conductor model of the midcervical spinal cord is shown in Fig. 1. This model of the spinal cord and its surrounding tissues consists of seven homogeneous compartments. They include the gray matter and white matter of the cord, the surrounding cerebrospinal fluid (csf) and at the dorsal side a thin layer, representing

Manuscript received May 27, 1992. This work was supported by a grant from Medtronic, Inc., Minneapolis, MN.

The authors are with the Institute for Biomedical Technology, Department of Electrical Engineering, University of Twente, Enschede, The Netherlands. IEEE Log Number 9209286.

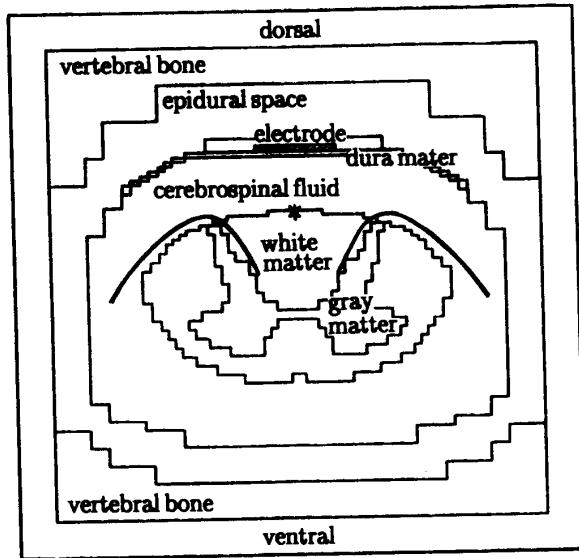


Fig. 1. Transverse section of the volume conductor model with two dorsal root fibers with curvature *A* (Fig. 4(a)); \* indicates the position of a dorsal column fiber used for the comparison of thresholds.

TABLE I  
CONDUCTIVITIES OF THE VOLUME CONDUCTOR COMPARTMENTS

Compartment	Conductivity (1/Ω m)
Gray matter	0.23
White matter	0.60 (longitudinal) 0.083 (transverse)
Cerebrospinal fluid	1.70
epidural space	0.040
Dura mater	0.020
Vertebral bone	0.040
Surrounding layer	0.0020 (bipolar stimulation) 0.010 (monopolar stimulation)

the dura mater and connective tissue between electrodes and dura. Between the vertebral bone and the dura mater (and csf) is the epidural space in which electrodes are placed at a dorsomedial position. The conductivities of the various compartments are presented in Table I. The values of the white matter, gray matter, epidural fat, and vertebral bone were taken from Geddes and Baker [10]. We measured the csf conductivity at 37°C previously in samples from three subjects [8]. Except for the white matter all conductivities are isotropic. The outer layer of the model has a low conductivity when stimulating bipolarly, thus approximating zero current flow to the boundary. In the monopolar case in which the zero voltage boundary serves as the distant anode, the surrounding layer conductivity is higher. All compartments are purely resistive because, even if the capacitive elements affect the pulse shape, this influence will be negligible as compared to the effect of the capacities in the nerve fiber models.

Because the dorsal rootlets have small diameters (less than 0.4 mm [11]), their volume will be small as compared to

the surrounding csf. Therefore, the dorsal rootlets were not modeled as separate compartments.

The dimensions of the cervical spinal cord model were the average values of data obtained from the literature [12]–[17]. The dorsoventral diameter was 7.6 mm and the lateral diameter was 13.6 mm. An important parameter is the dorsal csf-layer thickness, which is defined as the distance between the dorsomedial boundary of the spinal cord and the dura mater. Data on the thicknesses of the dorsal and ventral csf layer, obtained from a retrospective MRI and CT-scan study, were kindly supplied by G. Barolat and J. He.<sup>1</sup> From 23 subjects the average values of the dorsal and ventral csf-layer thickness at C4–C6 were 2.4 mm and 2.8 mm with standard deviations of 0.8 mm and 1.0 mm, respectively. The transverse shape of the cord and its divisions in white matter and gray matter were taken from Fix [11].

The volume conductor model was composed of 56 layers of volume elements in each (*x, y, z*) direction (making 56 × 56 × 56 elements). The variable layer thickness (0.2–4.0 mm) was chosen in such a way that the volume elements close to the electrodes and the dorsal columns of the spinal cord were smallest (0.2 mm). The dimensions of the model were 24.0 × 24.8 × 60.0 mm.

The flat electrodes were modeled as grid points with constant voltage (voltage sources). Monopolar and longitudinal bipolar (*z*-direction) electrode configurations were used. The electrode center-separation was 10 mm. The contacts were centered at *z* = 0 mm (monopolar) or *z* = –5.0 mm and *z* = 5.0 mm (bipolar). Electrode dimensions were 3.6 × 3.6 mm.

The potential field in this model was obtained by a finite difference technique using a Red-Black Gauss-Seidel iteration procedure [18] with a variable overrelaxation factor. The implementation was checked by comparing the analytically obtained field, due to a current point source in an infinite two-compartment medium (conductivity ratio = 1000), with the field calculated using the finite difference method in a finite medium. At the boundary of this finite medium the voltage values obtained by the analytical method were given. At more than five grid points away from the point source the error was less than 2%.

### III. NERVE FIBER MODELS

#### A. Dorsal Root Fibers

DR fibers and DC fibers are part of the same primary afferent fiber system. On entering the spinal cord the majority of DR fibers branch into an ascending and a descending DC fiber [19]–[21]. Many unmyelinated and small myelinated fibers enter the cord in Lissauer’s tract, while the larger myelinated fibers run into the lateral parts of the dorsal columns close to the dorsal horns [19]–[23] (Fig. 2). In comparison with the longitudinal DC fibers, the predominant features of DR fibers are their curved shape and their different orientation with respect to the cord and the electrodes.

<sup>1</sup>Thomas Jefferson Medical College, Philadelphia, PA.

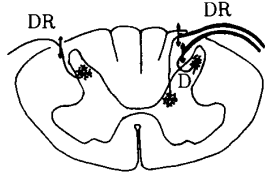


Fig. 2. Transverse section of the cervical spinal cord to show the entry of unmyelinated and thin myelinated dorsal root fibers (left side) as well as thick myelinated fibers (right side).



Fig. 3. Dorsal view of the spinal cord. At the left side the dorsal root filaments (rootlets) approaching the dorsal root entry zone are shown.

The dorsal root fans out in an ascending dorsomedial direction to form rootlets (Fig. 3), proximal to the dorsal root ganglion, which enter the spinal cord near to the dorsal horn [19]. As shown in Fig. 3 the rootlets of a single dorsal root enter the cord at different angles [24]. We supposed that in the midcervical region the angle varies from 0 to 45 degrees with respect to the transverse plane.

The position of a DR fiber in the volume conductor model was defined by a number of fiber definition points. The fiber trajectory was then calculated using cubic spline interpolated polynomials [25] for each of the coordinates  $x$ ,  $y$ , and  $z$  through the fiber definition points. The polynomials were used to calculate the coordinates of the nodes of Ranvier of the DR fiber, starting with the first node at the proximal end of the fiber and numerically solving  $s$  from the integral

$$nL = \int_0^s \sqrt{\left(\frac{dx}{du}\right)^2 + \left(\frac{dy}{du}\right)^2 + \left(\frac{dz}{du}\right)^2} \cdot du \quad (1)$$

where  $n$  is the node number ( $n = 0$  and  $s = 0$  at the proximal end),  $L$  the internodal length,  $s$  the parameter of the parametric curve ( $x = x(s)$ ,  $y = y(s)$ ,  $z = z(s)$ ). Note that in (1) the value of  $s$  has to be determined.

The various shapes of DR fiber models we used are presented in Fig. 4. The fiber model having a strong curvature in the transverse plane and a 45° angle with the transverse plane (fiber A1 in Fig. 4) was used as a standard fiber in our

simulations. The diameter of the standard DR fiber was 8  $\mu\text{m}$ , being in the lower range of the largest DR fibers [21].

The DR fiber model was sealed at its distal end, while at the proximal end the fiber was attached to a rostrocaudal DC fiber. This was done in the same way as attaching a collateral to a DC fiber (see below). The length of the fiber was such that the distal end was more than 10 nodes distant from the entry zone.

### B. Dorsal Column Fibers

The conduction velocity of a DC fiber close to the entry zone of the corresponding DR fiber is about 19% less than the conduction velocity of the DR fiber [26]. Assuming a linear relationship between fiber diameter and conduction velocity [27], we chose a DC fiber diameter of 6.4  $\mu\text{m}$ , being 80% of the DR fiber diameter used in this study.

DC fibers differ from simple straight nerve fibers because they issue collaterals perpendicular to the rostrocaudal main fiber, which run in a ventral direction into the gray matter (Figs. 2 and 5(a)). The model of this branched fiber (Fig. 5(b)) has been described by Struijk *et al.* [7].

Both the DR fibers and DC fibers were modeled as cable networks similar to McNeal's model [9], but with all nodes made excitable. The network (Fig. 5(b), for the DR fiber only the horizontal part of this figure) consists of membrane resistances ( $R_M$ ), membrane capacitances ( $C_M$ ), and intra-axonal resistances ( $R_a$ ) (see [7]). The nodal membrane kinetics were described by the equations given by Chiu *et al.* [28]. The external potentials at the nodes of Ranvier, serving as voltage sources in the fiber model, were obtained from the potential field calculated in the volume conductor model. Geometrical parameter values of the fiber models are given in Table II.

In Fig. 1 the position of the DC fiber model is indicated (\*). At this medial position at the dorsal column boundary, the threshold stimulus will be lower than those of a fiber deeper into the dorsal columns or at a more lateral position [29]. In one case a DC fiber was placed at the DR fiber entry point in the dorsal columns.

We calculated the threshold stimulus  $V_{th}$  for the excitation of DR fiber models to assess the influence of several fiber parameters and the thickness of the dorsal csf layer and electrode configuration in the volume conductor model. The fiber parameters were curvature, diameter, nodal position relative to the spinal boundary and rostrocaudal level of the DR fiber relative to the electrode(s). Thresholds of DR fibers were compared with those of a DC fiber (diameter 80% of the DR fiber diameter) at the dorosomedial boundary of the cord, issuing collaterals.

In all simulations single rectangular monophasic pulses with pulse durations of 210  $\mu\text{s}$  were used in both monopolar and bipolar electrode configurations.

## IV. RESULTS

### A. Influence of the Rostrocaudal Level of the DR Fiber on Threshold Stimulus

In order to assess the influence of the rostrocaudal level  $z$ , the DR fiber type A1 (Fig. 4) was used. The 8- $\mu\text{m}$  fiber

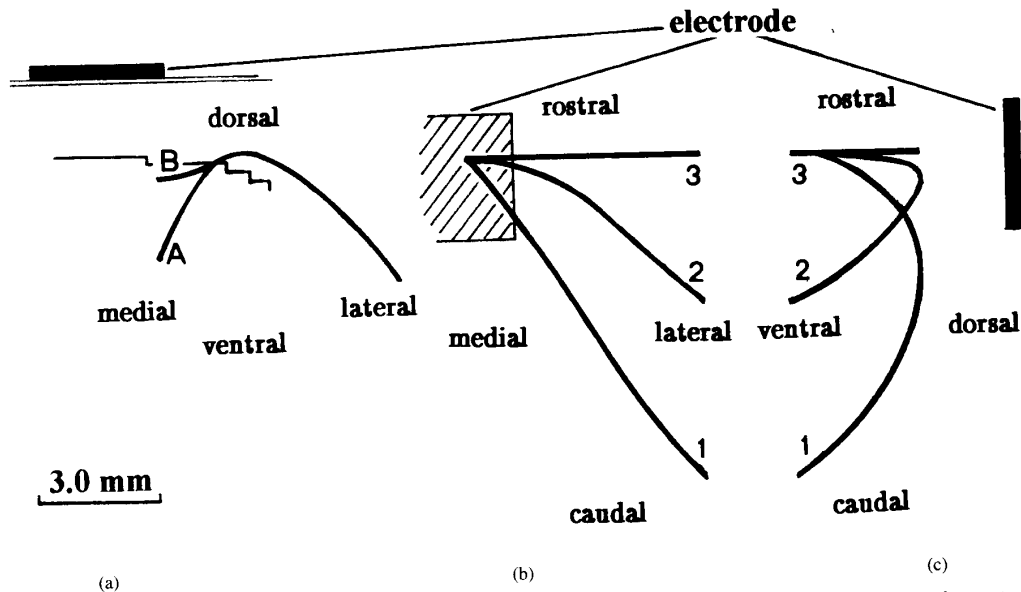


Fig. 4. Projections of the trajectories of curved dorsal fibers in three orthogonal planes. (a) Strong curvature *A* and weak curvature *B* in a transverse plane; (b) 45° (1) and 0° (2) curved fibers and horizontal fiber (3) in a coronal plane; (c) the same fibers as in (b) but in a sagittal plane and with curvature *B* in (a).

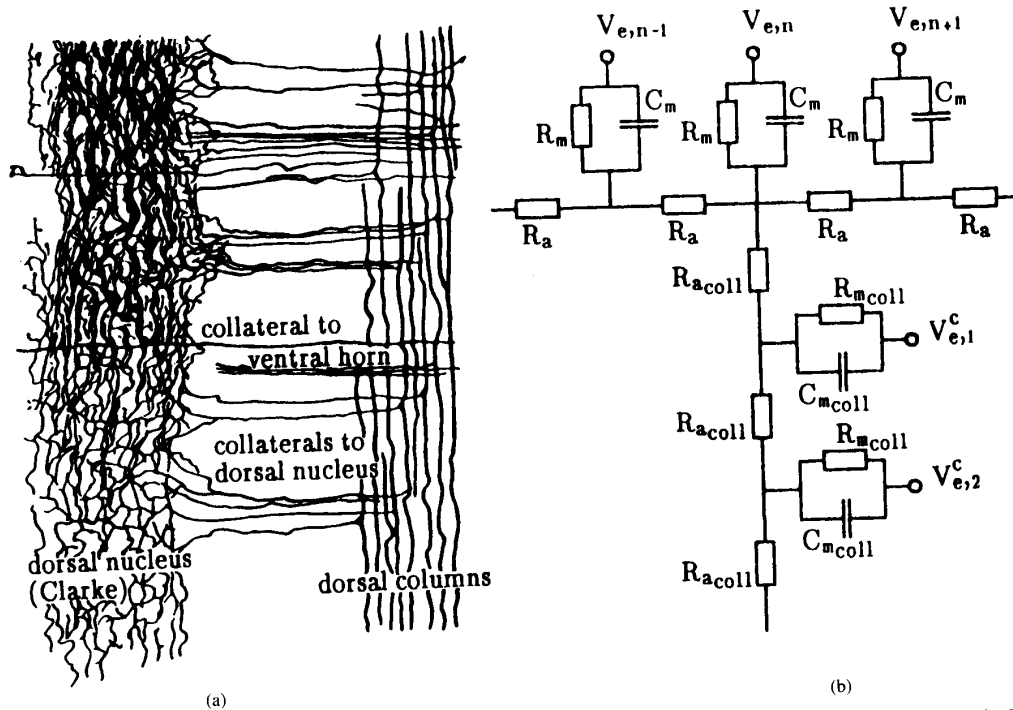


Fig. 5. Dorsal column fibers. a) Rostrocaudal DC fibers with collaterals running into the gray matter; b) network model of a DC fiber consisting of a rostrocaudal fiber (horizontal part) and a collateral (vertical part);  $R_m$ : nodal membrane resistance,  $C_m$ : nodal membrane capacitance,  $R_a$ : internodal intracellular resistance,  $V_e$ : nodal extracellular potential.

was positioned such that a node of Ranvier was exactly at the dorsal border of the cord. The volume conductor model (dorsal csf-layer thickness 2.4 mm) was used together with a bipolar electrode configuration with a rostral cathode (centered at  $z = 5$  mm, see Fig. 6).

The solid line in Fig. 6 shows the threshold stimulus ( $V_{th}$ ) as a function of the rostrocaudal level of the DR fiber. The rostrocaudal level was defined as the level at which the fiber crosses the dorsal boundary of the cord. The minimum value of  $V_{th}$  (4.68 V) was obtained at the rostrocaudal level of

TABLE II  
GEOMETRICAL PARAMETERS OF THE DC FIBER MODEL

Diameter of main fiber	6.4 $\mu\text{m}$
Diameter of collaterals	2.2 $\mu\text{m}$
Inner fiber diameter	0.6 $\times$ fiber diameter
Nodal Length	1.5 $\mu\text{m}$
Nr of nodes of main fiber	61
Nr of nodes per collateral	9
Nr of collaterals	15
Internodal length	100 $\times$ fiber diameter
Collateral spacing	2 $\times$ internodal length (=1.32 mm)
Termination	Sealed end

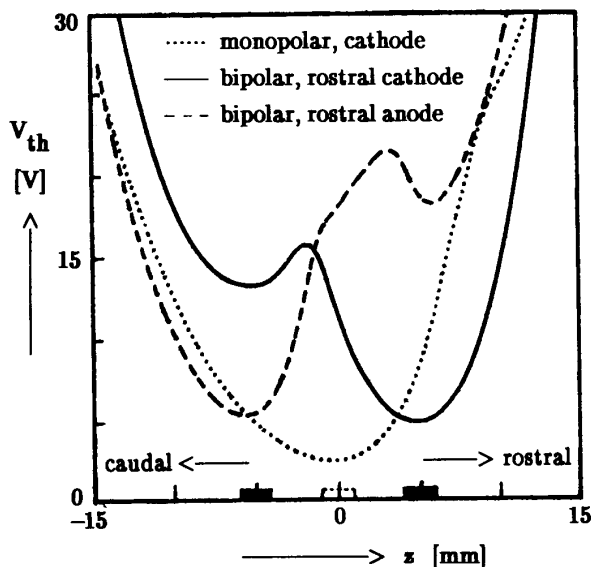


Fig. 6. Excitation thresholds  $V_{th}$  of the DR fiber A1 (Fig. 4) as a function of the rostrocaudal level  $z$  relative to electrodes, for monopolar and bipolar electrode configurations.

the cathode. The action potential was initiated at the node of Ranvier at the dorsal boundary. An 8- $\mu\text{m}$  rostrocaudal DC fiber at the same (transverse) position had a  $V_{th}$  of 9.86 V. The difference in threshold stimulus is caused by three properties in which DC fibers and DR fibers differ: 1) the fiber orientations with respect to the electrodes are different; 2) the DR fiber is curved while the DC fiber is straight; 3) the DR fiber crosses the interface between a low-conductivity and a high-conductivity compartment. All these properties contributed to the relatively low threshold of the DR fiber (see Sec. V, Discussion).

Near the anode a local minimum of  $V_{th}$  (13.14 V) occurred (Fig. 6, solid line). The node at which excitation was elicited was two or three nodes proximal to the one that was excited first at the cathodal level. Thus, at the anodal level excitation occurred at a node where the fiber has a more dorsoventral orientation (Fig. 1), which is in accordance with results from our previous work [7], [8]. The anodal  $V_{th}$  was 2.8 times the cathodal value.

TABLE III  
MINIMUM THRESHOLD STIMULI OF BOTH TYPE A1 DR FIBER ( $V_{DR}$ ) AND DORSOMEDIAL DC FIBER  $V_{DC}$  AND FIBER TYPE SELECTIVITY ( $S$ )

Dorsal csf-layer thickness [mm]	$V_{DR}$ [V]	$V_{DC}$ [V]	$S$
1.2	2.98	2.58	-0.07
2.4	4.68	5.60	0.09
3.6	6.94	10.50	0.20

### B. Influence of the Electrode Configuration on Threshold Stimulus

Changing the polarity of the bipolar configuration (rostral anode) did not merely mirror the function  $V_{th}(z)$  around  $z = 0$ , as shown in Fig. 6 (dashed line). From this figure it can be seen that the minimum  $V_{th}$  is still near the cathodal level, but that this minimum (5.18 V) is 10% higher than in the opposite electrode polarity. The local minimum near the rostral anode was 17.98 V, which is 37% higher than with a caudal anode and 11% higher than with a rostral cathode. The difference between the bipolar configurations is caused by the rostrocaudal asymmetry of the DR fiber trajectory (type A1).

When stimulating monopolarly (dotted line, Fig. 6) it is shown that  $V_{th}$  as a function of the rostrocaudal level  $z$  is also asymmetrical due to the rostrocaudal asymmetry of the DR fiber.

If the excitation length of an electrode configuration is defined as the length of the spinal segment at which type A1 DR fibers will be excited at a stimulus amplitude of twice the minimum  $V_{th}$ , then the monopole had an excitation length of 8.7 mm, whereas both bipolar configurations had an excitation length of 7.2 mm. Therefore, in our model the bipolar configurations had an approximately 20% higher spatial selectivity in DR fiber stimulation.

We defined fiber type selectivity ( $S$ ) of an electrode configuration as  $S = (V_{DC} - V_{DR}) / (V_{DC} + V_{DR})$ , where  $V_{DR}$  is the minimum threshold stimulus of the type A1 DR fiber (8  $\mu\text{m}$  diameter) and  $V_{DC}$  the threshold stimulus of a DC fiber (6.4  $\mu\text{m}$ ) at the dorsomedial boundary of the dorsal columns. So,  $S = 1$  if only DR fibers can be excited and  $S = -1$  if only DC fibers can be excited.  $S$  thus indicates which fibers are likely to be excited first, but  $S$  does not indicate the number of DC fibers vs. DR fibers that are excited. The monopole had a fiber type selectivity  $S = 0.13$  ( $V_{DC} = 3.10$ ,  $V_{DR} = 2.40$ ) whereas the bipolar configurations had selectivities  $S = 0.09$  ( $V_{DC} = 5.60$ ,  $V_{DR} = 4.68$ ) and  $S = 0.03$  ( $V_{DC} = 5.60$ ,  $V_{DR} = 5.26$ ) for the configurations with a rostral cathode and a rostral anode, respectively. In this case the monopole is the more selective one, although none of the configurations has a high fiber selectivity ( $S$  is close to zero).

### C. Influence of Dorsal Csf-layer Thickness on Threshold Stimulus

In Table III the threshold stimuli of a type A1 DR fiber (8  $\mu\text{m}$  diameter) and a DC fiber (6.4  $\mu\text{m}$ , dorsomedial boundary) are given for the bipolar configuration (rostral cathode) and a csf-layer thickness of 1.2 mm, 2.4 mm and 3.6 mm.

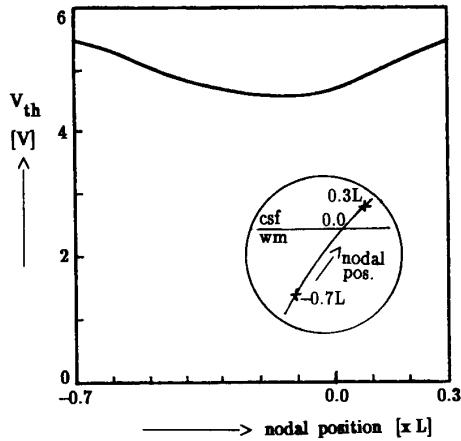


Fig. 7. Excitation thresholds  $V_{th}$  of the DR fiber A1 (Fig. 4) as a function of the position of the least threshold node of Ranvier. The nodal position is given as a fraction  $x$  of the internodal length  $L$ ; csf is the cerebrospinal fluid, wm is white matter.

Both the threshold stimuli of the DR fiber ( $V_{DR}$ ) and of the DC fiber ( $V_{DC}$ ) increased rapidly with increasing csf-layer thickness. However, at least a csf-layer thickness of 1.2 mm  $V_{DC}$  was lower than  $V_{DR}$ , whereas at a larger csf-layer thickness  $V_{DC}$  was higher. This  $V_{DC}$  to  $V_{DR}$  relation occurs because the distance between electrode and DC fiber is much smaller than the distance between electrode and DR fiber in case of a small thickness of the csf layer. With increasing csf-layer thickness the difference between the distances becomes proportionately less. Therefore, with increasing csf-layer thickness a DC fiber will have a larger relative increase of  $V_{th}$  than a DR fiber, resulting in a change of fiber type selectivity, as shown in Table III.

#### D. Influence of Nodal Position on Threshold Stimulus

In Fig. 7 the threshold stimulus  $V_{th}$  is drawn as a function of the position of the node at which the excitation was elicited. Again a bipolar electrode configuration with rostral cathode and a csf width of 2.4 mm were used. DR fiber diameter was 8  $\mu\text{m}$  and the rostrocaudal level of the lowest threshold node at the dorsal border of the cord was  $z = 5$  mm (cathodal level). This node was moved along the fiber in both proximal and distal directions until an adjacent node was excited first, which occurred when the nodes were displaced proximally by 70% of the internodal length ( $L$ ) (position =  $-0.7 \cdot L$ ). Consequently, the adjacent node at the opposite side was first excited when the nodes were moved in a distal direction along the fiber by 30% of the internodal length  $L$  (position =  $0.3 \cdot L$ ). The threshold varied between 4.45 and 5.48 V, (a variation of 23%) while varying the nodal position. The minimum  $V_{th}$  was at a nodal position of  $-0.15 \cdot L$ , just underneath the spinal surface.

#### E. Influence of Fiber Diameter on Threshold Stimulus

The influence of the fiber diameter on the minimum  $V_{th}$  was assessed for diameters in the range of 2 to 16  $\mu\text{m}$  (fiber type A1). The transverse position of the lowest threshold node

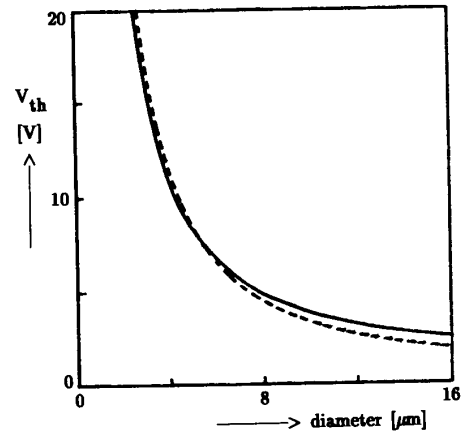


Fig. 8. Solid line: Excitation threshold of the DR fiber A1 (Fig. 4) as a function of fiber diameter; dashed line: excitation threshold of the dc fiber as a function of fiber diameter.

was 0.0 (at the dorsal boundary of the cord, Fig. 7) and its rostrocaudal level was  $z = 5$  mm (cathode level). The results are summarized in Fig. 8 (solid line). The threshold varies from 25.4 V for a 2- $\mu\text{m}$  fiber to 2.42 V for a 16- $\mu\text{m}$  fiber. Therefore, it seems improbable that small myelinated DR fibers will be excited in ESCS. The diameter dependency is because of the assumed relationship  $L = 100 \cdot d$  (see Table II), since the distance  $L$  between adjacent nodes of Ranvier is linear with fiber diameter  $d$  and the activating function [30] (which is a first-order approximation of the nodal transmembrane potential) usually increases with increasing internodal distance.

The thresholds of DC fibers at the dorsomedial boundary of the cord are also given in Fig. 8 (dashed line). DC fibers with a diameter less than 5  $\mu\text{m}$  have a higher threshold than DR fibers of the same fiber, while larger diameter DC fibers have a lower threshold. However, differences are small and so is the fiber type selectivity.

#### F. Influence of DR Fiber Curvature on Threshold Stimulus

Four DR fibers with different trajectories were compared with respect to their minimum value of  $V_{th}$ : A1, A2, A3, and B1 (Fig. 4). The lowest threshold node of Ranvier was at the dorsal boundary of the entry zone in all four cases. The minimum  $V_{th}$  values are presented in Table IV. From this table it can be concluded that the shape in a rostrocaudal direction has a significant influence in  $V_{th}$ . In particular, the angle at which the DR fiber approaches the dorsal root entry zone of the spinal cord seems to be important:  $V_{th}$  increases with increasing angle between the nerve fiber and the transverse plane. Because of its curvature, fiber A2 has a slightly lower  $V_{th}$  than the straight A3.

The difference in  $V_{th}$  between A1 and B1 illustrates the significance of the curvature in a transverse plane. A1, having a stronger curvature than B1, has by far the lowest threshold.

## V. DISCUSSION

The results of this study predict that under many conditions dorsal root fibers will have lower thresholds than

TABLE IV  
THRESHOLD STIMULUS  $V_{TH}$  FOR DIFFERENT DORSAL ROOT FIBER TYPES  
See Fig. 4.

DR Fiber	$V_{th}$ [V]
A1	4.68
A2	3.70
A3	3.76
B1	7.52

dorsal column fibers, although a small csf-layer thickness was shown to have lower  $V_{th}$  for dorsomedial DC fibers. Clinical experience shows that the medial DC fibers can be activated first, because in some cases paresthesia starts at a dermatome corresponding to a spinal level caudal to the position of the stimulating electrodes. However, usually initial paresthesiae were localized in dermatomes corresponding with the level of the electrodes and spread to caudal levels with increasing stimulus amplitude [31]–[33]. The initial segmental effects may be caused by activation of DR fibers in the dorsal root filaments or in the dorsal root entry zone, or to activation of the lateral DC fibers close to their entry level. If the csf-layer thickness is not too small, the lateral DC fibers have a lower threshold than the medial ones because the former have a larger diameter and a larger number of collaterals [7], [29]. This finding turned out to be more important than the difference in electrode-fiber distance of lateral and medial DC fibers. We concluded that the segmental effects could be the result of both DR fiber and lateral DC fiber stimulation, as far as sensory phenomena are concerned. Regarding motor effects, which are usually segmental [4], it is likely that dorsal root fibers are involved.

The properties of DR fibers emphasized by Coburn [6] were their curvature in a transverse plane and their diameter. In the present study we have found that the fiber orientation in a coronal plane, in combination with the rostrocaudal level relative to the electrodes, was important as well. This finding suggests that fibers of the same type in different rootlets of the same dorsal root may have different values of  $V_{th}$ .

Three properties of DR fibers were suggested to be responsible for their low  $V_{th}$ : their curvature, their orientation, and the fact that they cross the interface of two compartments having different conductivities.

1) The curvature of a fiber may change its  $V_{th}$  because with different curvatures the external potential field along the fiber will have a different second order difference (or activating function [30]). The activating function is a measure for the change of current density along the fiber, and is the source term of the differential equations describing the model of nerve fiber stimulation. The activating function is influenced by the fiber curvature [6]. If the fiber is bent away from the cathode, a decrease of  $V_{th}$  will result, whereas an opposite curvature will increase  $V_{th}$ . Therefore,  $V_{th}$  of DR fibers will be affected by their curvature.

2) The increasing threshold with decreasing angle between DR fiber and spinal cord axis can be explained by the fact that in the dorsal csf layer the dorso ventral activating function has a larger value than the rostrocaudal one [8]. Therefore,

the fibers having a dorsoventral orientation will have a lower threshold than fibers having a more rostrocaudal orientation.

3) The root filaments, immersed in the well-conducting csf, enter the spinal cord which has a lower conductivity (see Table I). The potential field gradient along the DR fiber increases largely upon entering the spinal cord [8] because of the sudden decrease of conductivity. Therefore, the activating function will be relatively high near the entry point, resulting in the initiation of fiber excitation at a node close to this point. It might be expected that the position of the node relative to the boundary would therefore be critical, but this was not the case, as was shown in our simulations.

The rootlets were not incorporated as separate compartments in the volume conductor model because they are small and are surrounded by the well-conducting, shunting csf. The rootlets will thus only have a minor influence on the potential distribution. In Coburn's work [6] the rootlets were exaggerated and were continuous along the whole rostrocaudal length of the volume conductor model.

Cathodal stimulation is well known to result in a lower threshold than anodal stimulation. In our model the DR fibers also have lower thresholds with cathodal stimulation. From this study it follows that anodal excitation occurs at a level about three times higher than the cathodal threshold.

A source of error in the calculations is the discretization of the governing Laplace equation. Large local errors may result, especially at compartment interfaces where large changes of conductivity occur. However, halving the grid spacing at the boundary of the dorsal root entry zone only gave rise to a change of  $V_{th}$  of an 8  $\mu\text{m}$  A1 fiber of less than 1%. If, in the bipolar case, the conductivity of the surrounding layer was changed, the change of the potential field was negligible and therefore the boundary conditions did not introduce any large errors.

The modeling results indicate that DR fibers are activated first and are followed by DC fibers at higher stimulus amplitudes. These results are supported by the clinical observation that initial effects are usually purely segmental. Therefore, we suggest not using the obviously confusing circumscription "dorsal column stimulation," which is often found in literature

## REFERENCES

- [1] C. N. Shealy, J. Th. Mortimer, and J. B. Reswick, "Electrical inhibition of pain by stimulation of the dorsal columns: Preliminary clinical report," *Anesthesia and Analgesia—Current Researches*, vol. 46, pp. 489–491, 1967.
- [2] C. N. Shealy, J. Th. Mortimer, and N. R. Hagfors, "Dorsal column electroanalgesia," *J. Neurosurg.*, vol. 32, pp. 560–564, 1970.
- [3] G. Barolat, "Epidural spinal cord stimulation in the management of spasms and spasticity in spinal cord injury," *Neurosurgery: State of the art reviews*, vol. 4, pp. 365–370, 1989.
- [4] M. R. Dimitrijevic, J. Faganel, P. C. Sharkey, and A. M. Sherwood, "Study of sensation and muscle twitch responses to spinal cord stimulation," *Int. Rehab. Med.*, vol. 2, pp. 76–81, 1980.
- [5] H. Bantli, J. R. Bloedel, D. M. Long and P. Thienprasit, "Distribution of activity in spinal pathways evoked by experimental dorsal column stimulation," *J. Neurosurg.*, vol. 42, pp. 290–295, 1975.
- [6] B. Coburn, "A theoretical study of epidural electrical stimulation of the spinal cord—Part II: Effect on long myelinated fibers," *IEEE Trans. Biomed. Eng.*, vol. 32, pp. 978–986, 1985.
- [7] J. J. Struijk, J. Holsheimer, G. G. van der Heide, and H. B. K. Boom, "Recruitment of dorsal column fibers in spinal cord stimulation:



Influence of collateral branching," *IEEE Trans. Biomed. Eng.*, vol. 39, pp. 903-912, 1992.

[8] J. J. Struijk, J. Holsheimer, B. K. van Veen, and H. B. K. Boom, "Epidural spinal cord stimulation: Calculation of field potentials with special reference to dorsal column nerve fibers," *IEEE Trans. Biomed. Eng.*, vol. 38, pp. 104-110, 1991.

[9] D. R. McNeal, "Analysis of a model for excitation of myelinated nerve," *IEEE Trans. Biomed. Eng.*, vol. 23, pp. 329-337, 1976.

[10] L. A. Geddes and L. E. Baker, "The specific resistance of biological material—a compendium of data for the biomedical engineer and physiologist," *Med. Biol. Eng.*, vol. 5, pp. 271-293, 1967.

[11] J. D. Fix, *Atlas of the Human Brain and Spinal Cord*. Rockville, MD: Aspen Publishers, 1987.

[12] C. H. Elliot, "cross sectional diameters and areas of the human spinal cord," *Anat. Rec.*, vol. 93, pp. 287-293, 1945.

[13] L. Nordqvist, "The sagittal diameter of the spinal cord and subarachnoid space in different age groups: A roentgenographic study," *Acta Radiologica*, suppl. 227, pp. 1-96, 1964.

[14] L. Penning, J. T. Wilmink, H. H. van Woerden, and E. Knol, "CT-myelographic findings in degenerative disorders of the cervical spine: Clinical significance," *Amer. J. Radiol.*, vol. 146, pp. 793-801, 1986.

[15] H. O. M. Thijssen, A. Keyser, M. W. M. Horstink, and E. Meijer, "Morphology of the cervical spinal cord on computed tomography," *Neuroradiol.*, vol. 18, pp. 57-62, 1979.

[16] I. O. Skälpe and O. Sortland, "Cervical myelography with metrizamide (amipaque) *Neuroradiol.*" vol. 16, pp. 275-278, 1978.

[17] J. L. Sherman, P. Y. Nassaux, and C. M. Citrin, "Measurement of the normal cervical spinal cord on MR imaging," *Amer. J. Radiol.*, vol. 111, pp. 369-372, 1990.

[18] G. Dahlquist and O. Björck, *Numerical Methods*. Englewood Cliffs, NJ: Prentice-Hall, 1974.

[19] M. B. Carpenter, *Core Text of Neuroanatomy*. Baltimore: Williams & Wilkins, 1972.

[20] A. R. Light, "Normal anatomy and physiology of the Spinal Cord dorsal horn," *Appl. Neurophysiol.*, vol. 51, pp. 78-88, 1988.

[21] R. E. W. Fyffe, "Afferent fibers," in *Handbook of the Spinal Cord*, vols. 2 and 3, *Anatomy and Physiology*, R. A. Davidoff, ed. New York: Dekker, 1984, pp. 79-136.

[22] R. Snyder, "The organization of the dorsal root entry zone in cats and monkeys," *J. Comp. Neur.*, vol. 174, pp. 47-70, 1977.

[23] S. T. Bok, "Das Zentralnervensystem: Das Rückenmark," in *Handbuch der mikroskopischen Anatomie des Menschen*, vol. 4. Berlin: Springer-Verlag, 1928, pp. 478-578.

[24] R. y Cajal, "Histologie du Système Nerveux de L'homme et des Vertébrés." vol. I, Paris, 1912.

[25] J. Stoer and R. Bulirsch, "Introduction to Numerical Analysis." New York, NY: Springer-Verlag, 1980.

[26] J. E. Desmedt and G. Cheron, "Central somatosensory conduction in man: Neural generators and interpeak latencies of the far field components recorded from neck and right or left scalp and ear lobes," *Electroencephalgr. Clin. Neurophysiol.*, vol. 50, pp. 382-403, 1980.

[27] A. S. Paintal, "Conduction properties of normal peripheral mammalian axons," in *Physiology and Pathobiology of Axons*, S. G. Waxman, Ed. New York: Raven Press, 1978.

[28] S. Y. Chiu, J. M. Ritchie, R. B. Rogart, and D. Stagg, "A quantitative description of membrane currents in rabbit myelinated nerve," *J. Physiol.*, vol. 292, pp. 149-166, 1979.

[29] J. Holsheimer, J. J. Struijk, and N. J. M. Rijkhoff, "Contact combina-

tions in epidural spinal cord stimulation: A comparison by computer modeling," *Stereotact. Funct. Neurosurg.*, vol. 56, pp. 220-233, 1991.

[30] F. Rattay, "Analysis of models for external stimulation of axons," *IEEE Trans. Biomed. Eng.*, vol. 33, pp. 974-977, 1986.

[31] L. S. Illis, E. M. Sedgwick, and R. C. Tallis, "Evaluation of possible mechanisms of action of spinal cord stimulation," in *Proc. 6th Int. Symp. Extern. Contr. Human Extremities*, Dubrovnic, pp. 647-656, 1978.

[32] G. Barolat, S. Zeme, and B. Ketcik, "Multifactorial analysis of epidural spinal cord stimulation," *Stereotact. Funct. Neurosurg.*, vol. 56, pp. 77-103, 1991.

[33] J. D. Law, "Spinal stimulation: Statistical superiority of monophasic stimulation of narrowly separated longitudinal cathodes," *Appl. Neurophysiol.*, vol. 46, pp. 129-137, 1983.



**Johannes J. Struijk** was born in Rijssen, The Netherlands, in 1963. He received the M.Sc. degree in electrical and biomedical engineering in 1988 and the Ph.D. degree in 1992 from the University of Twente, The Netherlands.

He is currently employed in the Biomedical Engineering Division of the Dept. of Electrical Engineering, Univ. of Twente. His current research activities are related to stimulation of nervous tissue and involve volume conduction and neural modeling.



**Jan Holsheimer** was born in Enschede, The Netherlands in 1941. He received the M.Sc. degree in biology and biophysics from the University of Groningen, The Netherlands in 1965 and the Ph.D. degree in biomedical engineering from the University of Twente, The Netherlands, in 1982.

In 1965 he joined the Biomedical Engineering Division, Dept. of Electrical Engineering, Univ. of Twente. His research interests are volume conduction and the analysis of field potentials in the brain and electrical stimulation of nervous tissue.



**Herman B. K. Boom** was trained as a medical physicist at the University Utrecht, The Netherlands, where he received the Ph.D. degree in 1971.

He joined the Departments of Medical Physics and Medical Physiology where he was engaged in research in the field of cardiac mechanics and taught physiology and biophysics. Since 1976 he has held the Chair of Medical Electronics in the Dept. of Electrical Engineering, Univ. of Twente, The Netherlands. His research interests are cardiovascular system dynamics, bioelectricity and reha-

bilitation technology.